Atmospheric Research 283 (2023) 106545

Contents lists available at ScienceDirect

Atmospheric Research

journal homepage: www.elsevier.com/locate/atmosres

Performance of CHIRPS dataset for monthly and annual rainfall-indices in Northern Argentina

Franco D. Medina [a,b,*], Bruno S. Zossi [a,b], Adriana Bossolasco [a,b], Ana G. Elias [a,b]

[a] LIANM, Departamento de Física, Facultad de Ciencias Exactas y Tecnología, Universidad Nacional de Tucuman, Tucumán 4000, Argentina
[b] INFINOA (CONICET-UNT), Tucuman 4000, Argentina

ARTICLE INFO

Keywords:
CHIRPS
Argentina
Interannual variability
Trends
Satellite

ABSTRACT

In this study, we analyze the performance of CHIRPS in comparison with data from 50 rain gauges (OBS) in Northern Argentina (NA) for the 1982–2019 period. The methodology consists in a point-to-pixel comparison using the correlation coefficient (RHO), the mean relative error (MRE), the mean absolute error (MAE) and the Nash-Sutcliffe efficiency (NSE). We analyze monthly rainfall, annual rainfall indices and their trends, differentiating between anchor and no-anchor stations. A comparative analysis is performed further between two NA sub-regions: Northwestern Argentina (NWA) and Northeastern Argentina (NEA). Results indicate that CHIRPS dataset better represents the interannual variability in wetter (drier) months in NWA (NEA). For all months, RHO values are higher in NEA than NWA. For annual rainfall indices, RHO values in most of the stations of NA are non-significant or low for some number-days (with threshold of 1 mm) and very extreme indices, with the exception of the eastern extreme of NA. The less extreme indices (PRCPTOT, R95pad and R99pad) are observed to have higher RHO values (> 0.5 in all cases) in NA, as well as better MRE, MAE and NSE values. Monthly values and annual indices are underestimated in general, especially in NWA no-anchor stations. Most of the significant linear trends observed in rainfall indices are not detected with CHIRPS. As an exception, a relatively better performance for the maximum number of consecutive dry days (CDD) is observed in the sense that CHIRPS detect the positive linear trends in NWA but do not locate them with precision in comparison with OBS data. CHIRPS is not recommended for studies in NA related with the aspects (mean values, interannual variability, linear trends) of rainfall analyzed in this work, especially for the extreme rainfall.

1. Introduction

Rainfall is a key component of many natural systems, such as agriculture and hydrology, which are fundamental to society and economy. In particular, its excess or deficit can lead to material and even life losses. With global warming, rainfall extremes are intensifying at a rate consistent with the increase in atmospheric moisture (Fowler et al., 2021), and in addition, the risk of droughts will increase (Xu et al., 2019). According to the World Meteorological Organization (WMO) (2021) disasters associated with rainfall or drought events have implied, since 1970, the death of >1 million people with >91% of these deaths occurring in developing countries. At the same time, economic losses from weather-related disasters increased around seven times. Thus, continuous monitoring of rainfall is crucial for forecasts that would allow adequate prevention and mitigation measures planned in advance. Furthermore, the availability of high-resolution gridded rainfall datasets is a prerequisite for disaster risk reduction and management (Shrestha et al., 2021) considering that extreme rainfall indices are based on daily records which can have strong spatial gradients. Gridded rainfall datasets with coarser resolution would fail to detect critical small scale features.

Among different rainfall data sources, gridded data are preferred due to its advantage of uniform coverage around vast regions of the world. These datasets can be gauge, reanalysis or satellite-based, where each can cover distinct periods (in terms of both: length and dates) and also have different temporal and spatial resolutions. Each of these three types of datasets has deficiencies linked to the number and spatial coverage of surface stations in gauge-based case, the data assimilation models in the reanalysis-based case, and the satellite algorithms in the last case (Sun et al., 2018). In recent years the interest in rainfall data derived from

* Corresponding author at: LIANM, Departamento de Física, Facultad de Ciencias Exactas y Tecnología, Universidad Nacional de Tucuman, Av. Independencia 1800 - San Miguel de Tucumán, Tucumán, Argentina.
E-mail address: fdmedina@herrera.unt.edu.ar (F.D. Medina).

https://doi.org/10.1016/j.atmosres.2022.106545
Received 10 June 2022; Received in revised form 25 November 2022; Accepted 26 November 2022
Available online 30 November 2022

satellites has increased due to the wider spatial coverage that they offer. On the other hand, the accuracies of gridded precipitation datasets should be evaluated and examined in reference to ground observations, as these data can be affected by systematic errors (Faiz et al., 2018).

Between the available satellite-related datasets, the Climate Hazards Group InfraRed Precipitation with Station data (CHIRPS) stands out because of it has spatial and temporal coverage, latency, and resolution that is unprecedented for a global terrestrial product (Funk et al., 2015). The algorithm of CHIRPS incorporates daily, pentadal, and monthly 1981-present 0.05° estimates of precipitation based on infrared Cold Cloud Duration (CCD) observations and station data (Funk et al., 2015). Among CHIRPS' purposes are drought monitoring, rainfall detection, trend analysis and streamflow simulation. More details of the CHIRPS dataset can be found in Funk et al. (2015).

Validation studies of CHIRPS have been performed in the last years in many regions around the globe, e.g., Argentina, Brazil, Chile, Italia, China, among others (Funk et al., 2015; Baez-Villanueva et al., 2018; Rivera et al., 2018; Cavalcante et al., 2020; and references therein). In the Southern of South America, a study of Cerón et al. (2020) was performed in La Plata Basin (LPB) (Argentina, Brazil, Paraguay and Bolivia) finding that CHIRPS better represents the monthly rainfall in the east plain and coastal region than in the west Andean region. Further, as a strong point, CHIRPS describes most of the observed rainfall variability in the LPB, especially during December–February and March–May seasons. On the other hand, in the Central Andes of Argentina, results of Rivera et al. (2018) indicate that CHIRPS reproduce adequately the seasonal and interannual variability together with the spatial patterns of precipitation, but overestimates at higher elevations (above 1000 m) with a consequent performance decrease. This difference has been attributed in part to the limited number of stations to produce CHIRPS. Rivera et al. (2019) obtain further results for that region and state that CHIRPS is a suitable tool for assessing dry and wet conditions for timescales longer than one month and can support decision-making processes within the hydro-meteorological agencies. Likewise, Zambrano et al. (2017) analyzed rainfall measurements across Chile finding that, overall, CHIRPS was a useful dataset for characterizing precipitation patterns in this country, providing also a valuable data source to calculate precipitation-based drought indices to monitor drought.

An interesting study of Cavalcante et al. (2020) in the Brazilian Legal Amazonia (BLA) compares monthly rainfall, annual rainfall indices and their trends calculated using CHIRPS and rain gauge observations. They found that in the BLA region, CHIRPS provided mean monthly rainfall similar to that obtained using data from the rain gauge stations. However, it has a poor performance for the most extreme indices and is not suitable for trend detection in this region.

In the present work, a validation study of CHIRPS performance in representing monthly total rainfall and annual extremes rainfall indices, together with their trends in North Argentina (NA) region is done, following the scheme of Cavalcante et al. (2020). Some NA stations used here are also used in the CHIRPS production, but we included others that are not incorporated for comparison.

Some related studies about rainfall in NA were performed, all of them based on gauge observations (Castino et al., 2017; Lovino et al., 2018; Ferrero and Villalba, 2019) or CHIRPS data (Cerón et al., 2021), separately. Only the study of Cerón et al. (2020) compares CHIRPS data with gauge observations in a region that encompasses most of NA region. The new contribution of this work is to extend this validation to annual extremes rainfall indices and trend detection in NA, in order to determine the feasibility of using CHIRPS for climatic studies related with rainfall variability and forecast in this region.

The relevance of understanding the variability, intensity, and distribution of precipitation particularly in NA is given by, on one hand, the great importance of the agricultural sector in the economy of the region (sugar cane, cereals, oilseeds and fruits). On the other, being able to anticipate the floods occurring during the rainy season due, among other things, to excessive logging in foothill areas of the region, where housing estates were built. In addition, there are unfortunately marginal population settlement areas on river banks that usually have large floods during extreme, and not so extreme, precipitation events. Without leaving aside either, that the urban area, in most populated NA provinces, has grown markedly in housing density during the last decades without any urban planning or strategy for city densification, so there was no accompaniment of the drainage infrastructure, for example. This means that there are also large floods with damaging consequences in these areas (Bello et al., 2018).

2. Study region

This study is carried out in the territory of 11 Argentine provinces located in the north of the country. The area encompasses the subtropical region between 21°S and 31°S and between 69°W and 53°W. It has an approximate surface area of 900,000 km^2, and almost 9 million inhabitants that is 20% of Argentina's total population (data from INDEC available at https://www.indec.gob.ar/indec/web/Nivel4-Tema-2-24-85). This region produces 13% of the Growth Domestic Product (data from INDEC available at https://www.indec.gob.ar/indec/web/Nivel4-Tema-3-9-138) in an economy mainly based in hydroelectric power and agricultural activities strongly depending on climate.

Two different sub-regions can be identified in NA: Northwestern (NWA) and Northeastern Argentina (NEA). In fact, the country is divided into five main regions according to climatic characteristics and productivity, two of which are precisely NWA and NEA. The boundaries between these regions follow the province's geographical limits, and in the case of these two regions, the boundary between them is, even though not exactly, almost a straight line at 62°W. In our case, the gauge stations considered are far from this limit and this imaginary straight line works properly dividing both regions in our study. The distinction between NWA and NEA is often used in studies that involve the NA region and it is related with the different rainfall regimes (Doyle, 2020, and references therein). We further checked these differences between NWA and NEA computing the annual cycle of rainfall for each station used in this work and for regional means (Fig. S1). Annual cycle is more marked in NWA where a greater concentration of rainfall in warmer months is observed in comparison with NEA, where the annual cycle is more flattened. Despite these differences, in general warmer months are rainier and colder months are drier in agreement with Cerón et al. (2020). Fig. 1 shows the location and main topographic features of NA, together with rain gauges used for the validation of satellite-based rainfall estimates distinguished between NWA and NEA stations using different colors (black symbols for NWA and red symbols for NEA). NWA is encompassed by the Andes Mountain Range, where rainier conditions are found in elevations between 300 and 3000 m and driest conditions in elevations above 3000 m (Castino et al., 2017). In contrast, NEA is mostly plain with elevations under 300 m and rainier conditions to the east (Lovino et al., 2018).

The NA region includes most of the locations with the highest rainfall values in the country (Llano, 2018). As can be noticed in Fig. 2, in the summer months (December to February), the maximum rainfall occurs in NWA and this is a result of the orography of the Andes (Bookhagen and Strecker, 2008). In summer, rainfall is regulated by the South-American Monsoon (Marengo et al., 2012). The circulation provides a water vapor flux from the Amazonas region and the tropical Atlantic Ocean through the low-level jet flux (Vera et al., 2006). Summer rainfall in NA is frequently organized in large mesoscale convective systems (Laing and Fritch, 2000). During the other seasons the low-level jet decays with the maximum rainfall occurring in NEA and mostly related to mean latitude synoptic scale activity (Vera et al., 2002). The interannual variability in NA is mainly associated to El Niño-Southern Oscillation (Barros et al., 2008; Cerón et al., 2020) and to the surface temperature gradient between the Atlantic and Pacific Oceans (Barreiro et al., 2014).

Trends in some rainfall indices were observed in the last seven

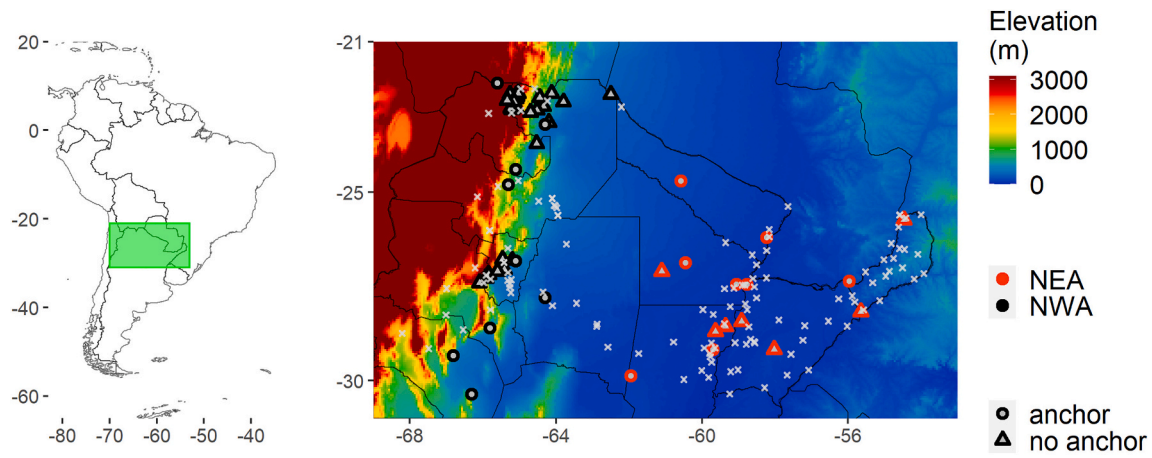

Fig. 1. NA location in South America (green rectangle). Further, location of the 50 stations included (anchor: circle, no-anchor: triangle; NWA: black symbols, NEA: red symbols), and the 120 stations not included (gray cross) in this study. Elevation of NA in meters above sea level is colored. (For interpretation of the references to colour in this figure legend, the reader is referred to the web version of this article.)

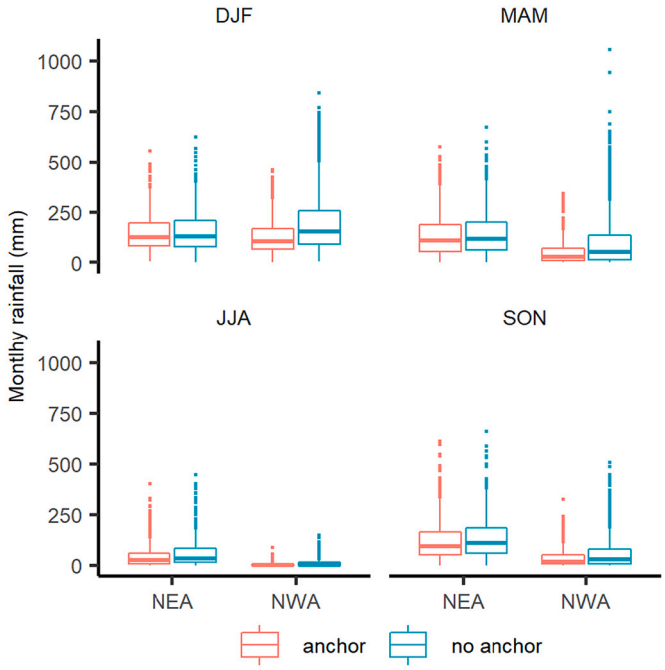

Fig. 2. Boxplot of seasonal rainfall values in the 1990–2019 period from OBS data separated by region (NWA and NEA) for anchor (pink) and no-anchor stations (blue). (For interpretation of the references to colour in this figure legend, the reader is referred to the web version of this article.)

decades in NA according to gauge data. Particularly, a review of Carvalho (2020) identified that NA (subtropics of South-America) is one of the two regions of America with the most consistent evidence of rainfall positive trends in the past century. However, in the last four decades, some differences with respect to this behavior were observed. For NWA a decrease was observed in the total annual rainfall and the frequency of wet days, but in contrast an increase of rainfall extremes related to the 95th percentile was observed (Castino et al., 2017). On the other hand, for NEA the occurrence of intense rainfall events increased steadily from 1970 up to 2000 with a stabilization trend since then, and at the same time a continuous increase in the duration of dry spells (Lovino et al., 2018). Thus, rainfall monitoring in the region is increasingly necessary due to the rainfall behavior is becoming more extreme.

3. Material and methods

As mentioned above, this work uses a similar methodology to that of Cavalcante et al. (2020), applied to the NA region. A point-to-pixel analysis is made to compare rainfall from CHIRPS and rain gauge stations' observations (OBS). This analysis consists in extracting the time series from CHIRPS database of the pixel closer to the location of each rain gauge station selected. Missing daily data in OBS is considered missing in CHIRPS for comparison. Monthly total rainfall and annual rainfall indices were compared using the following statistics: Pearson's linear correlation coefficient (RHO), the mean relative error (MRE), the mean absolute error (MAE) and the Nash-Sutcliffe efficiency (NSE), whose equations are listed in Table 1. That is, from the four statistics also used by Cavalcante et al. (2020) we only changed one: NSE instead of the mean error, considering the first gives more new information regarding the other three statistics used.

RHO measures the linear association strength between, in this particular case, CHIRPS and OBS, that is how similar is the variability in one series to that of another. It is bounded by 1 and − 1, where 1 is the optimal value indicating that both time series varies identically. The statistical significance of the RHO was determined using the Student's *t*-test to 0.05 level of significance. MRE measures the average bias of CHIRPS over or underestimating OBS depending on its sign: positive or negative, respectively. It gives similar information to the percentage bias, and its optimal value is 0. MAE is a scale-dependent measure of deviation that in this case corresponds to CHIRPS deviation from OBS. The optimal value is 0 indicating that both series are identical. NSE

Table 1
Equations for the statistical metrics to evaluate CHIRPS performance. CHIRPS and OBS are represented by x and y, respectively; n corresponds to the number of points.

Name	Equation
Pearson's correlation coefficient (RHO)	$RHO = \frac{n(\Sigma xy) - (\Sigma x)(\Sigma y)}{\sqrt{\left[n\Sigma x^2 - (\Sigma x)^2\right]\left[n\Sigma y^2 - (\Sigma y)^2\right]}}$
Mean relative error (MRE)	$MRE = \frac{1}{n}\Sigma\frac{(x-y)}{y}$
Mean absolute error (MAE)	$MAE = \frac{1}{n}\Sigma\lvert x-y\rvert$
Nash-Sutcliffe efficiency (NSE)	$NSE = 1 - \frac{\Sigma(x-y)^2}{\Sigma\left(x-\frac{\Sigma x}{n}\right)^2}$

determines the relative magnitude of the "residual variance" between CHIRPS and OBS (called residual for its analogy to regression analysis) compared to OBS variance (Nash and Sutcliffe, 1970). This statistic range from -∞ to 1. A negative value corresponds to a poor precipitation estimation by CHIRPS and implies that OBS mean value is a better predictor; 0 indicates that CHIRPS is as accurate as the mean; and 1 (the optimal value) implies a perfect match between CHIRPS and OBS.

The annual rainfall indices analyzed by Cavalcante et al. (2020) were also used in this study (Table 2). They selected those defined on the core set of ETCCDI descriptive indices of extreme precipitation (Karl et al., 1999), which are 11 out of a total of 27, plus two all-day percentiles, the number of days with rainfall, and the sum of precipitation of the 4 days with the highest rainfall, adding up to 15 indices. We included the same selection considering that, even though some of them may give redundant information, they are all relevant to climate change detection and measure aspects of frequency, duration and intensity meaningful to policy makers in NA region.

Trends in rainfall indices were estimated using the Sen's slope estimator (Sen, 1968) and the significance calculated with the modified nonparametric Mann-Kendall test (Hamed and Rao, 1998; Kendall, 1955; Mann, 1945) to 0.05 level of significance. Data from some rain gauge stations used here were included in CHIRPS production and are named "anchor" stations (circles in Fig. 1). Those not used in CHIRPS production are named "no-anchor" stations (triangles in Fig. 1). Unlike Cavalcante et al. (2020), we separate explicitly the analysis between anchor and no-anchor stations for comparison.

3.1. Rainfall data

Daily rainfall records provided by the Servicio Meteorológico Nacional (available under request), Subsecretaría de Recursos Hídricos (available online at www.argentina.gob.ar/subsecretaria-de-recursos-hidricos/base-de-datos-hidrologica-integrada) and Instituto Nacional de Tecnologia Agropecuaria (available online at siga.inta.gob.ar/) from Argentina are used. From a total of 170 rainfall stations in NA, the 50 selected for this study are listed in the Supplementary Material (Table S1). The density of stations is 0.056 stations per 1000 km^2, but they are unevenly distributed, as can be noticed in Fig. 1. Many stations are placed along main rivers, while others in the airports of the principal cities or important agricultural zones in NA. As in Cavalcante et al. (2020), we visually checked time series to detect obvious erroneous data. Further, for each month, monthly total accumulated rainfall, maximum daily rainfall and maximum consecutive days without rainfall that deviates four standard deviations or more respect to the monthly mean were compared with values of neighboring stations. Values suspected as erroneous were considered missing. Stations with <20% of monthly missing data in the 1982–2019 period were selected, considering missing those months with more than one-day missing. Some record beginning various years later of the 1982-year, however were selected because they had at least 80% of monthly data in the 1982–2019 period. Based on these criteria we discarded 120 stations out of the 170. Between the selected stations, the shortest period covered is 1989–2019 and the longest is 1982–2019. The major density of the stations is concentrated over Tucuman province in the center of NWA, where a strong elevation gradient exists. From the 50 selected stations, 35 are in NWA and 15 in NEA. For the computation of annual indices, we consider the year as NA hydrologic year which begins in July 1 and ends in June 30, since the maximum rainfall occurs in the warmer months.

Table 2
Description of the 15 rainfall indices used in this study.

Name	Description
nP	Number of days with R ≥ 1 mm
RX1DAY	Maximum 1-day precipitation
SDII	Simple precipitation intensity index: mean daily precipitation intensity of days with R ≥ 1 mm
RX5DAY	Maximum consecutive 5-day precipitation
R10MM	Count of days when $R \geq 10$ mm
R20MM	Count of days when $R \geq 20$ mm
R50MM	Count of days when $R \geq 50$ mm
CDD	Maximum length of dry spell: maximum number of consecutive days with $R < 1$ mm
CWD	Maximum length of wet spell: maximum number of consecutive days with R ≥ 1 mm
R95P	Total precipitation when $R >$ 95 percentile of days with $R \geq 1$ mm
R99P	Total precipitation when $R >$ 99 percentile of days with R ≥ 1 mm
R95pad	Total precipitation when R > 95 percentile of all days
R99pad	Total precipitation when R > 99 percentile of all days
PRCPTOT	Annual total precipitation
RTOP4	Sum of precipitation of the 4 days with highest R

3.2. CHIRPS data

Daily rainfall estimates from CHIRPS dataset version 2.0 (Funk et al., 2015) were used with a horizontal resolution of 0.05°. Data was downloaded from https://coastwatch.pfeg.noaa.gov/erddap/griddap/chirps20GlobalDailyP05.html. CHIRPS combines satellite measurements of Cloud Cold Duration (CCD) calibrated with Tropical Rainfall Measuring Mission (TRMM) 3B42 data and gauge station data. Previous to the CHIRPS production is derivate the satellite-only Climate Hazards group Infrared Precipitation (CHIRP) field. The primary computing time step for the CHIRP is the pentad. There are six pentads in a calendar month, five 5-day pentads and one pentad with the remaining 3 to 6 days, depending on month. Pentadal CHIRP values are disaggregated to daily precipitation estimates based on daily CFS (Coupled Forecast System reanalysis, version 2) fields, rescaled to 0.05° resolution. At each pixel, the CHIRP pentad total is redistributed in proportion to the daily values of the CFS. The final CHIRPS estimate is a combination of unadjusted and bias-adjusted CHIRP data. The result is a gridded daily product of rainfall with resolution of 0.05° that covers from −50° to 50° of latitude. Rivera et al. (2018) observe that in CHIRPS production is not included data from Argentinean agencies different from the Servicio Meterologico Nacional. We checked the list of the anchor stations (available in https://data.chc.ucsb.edu/products/CHIRPS-2.0/diagnostics/list_of_stations_used/) of CHIRPS and found that out of the 50 stations selected for this study 16 were incorporated. Of the 34 no-anchor stations, 26 correspond to NWA and 8 to NEA. We analyze separately anchor and no-anchor stations to avoid bias in the results of this validation study that can arise from a non-distinction of this condition.

4. Results

4.1. Monthly rainfall and annual indices from rain gauges

Fig. 2 shows the boxplots of seasonal rainfall for OBS data over the period 1990–2019, that is, for this figure we selected a 30-years period which is common to all the stations. From the boxplots it is clearly deduced that JJA (winter) is the driest season. The maximum seasonal rainfall in NA occurs in summer (DJF), and in particular in NWA no-anchor stations. Thus, NA rainiest stations are not incorporated in CHIRPS production. Furthermore, not only in DJF, but in all seasons, NWA no-anchor stations are rainier than anchor stations. In the case of NEA, the difference between anchor and no-anchor stations' seasonal rainfall is smaller.

The spatial distribution of OBS mean monthly rainfall over the period 1990–2019 is shown in Fig. 3. The maximum rainfall values are found in the center of NWA from December to March. A secondary maximum is observed during the same months in the east of NEA. In the other months, the maximum rainfall values occur in the east of NEA. In general, NA rainfall values are lower from May to August, denoting the existence of a dry season which is more evident in NWA than in NEA.

Mean annual rainfall indices estimated with OBS data over the period 1990–2019 are shown in Fig. 4. The case of PRCPTOT is

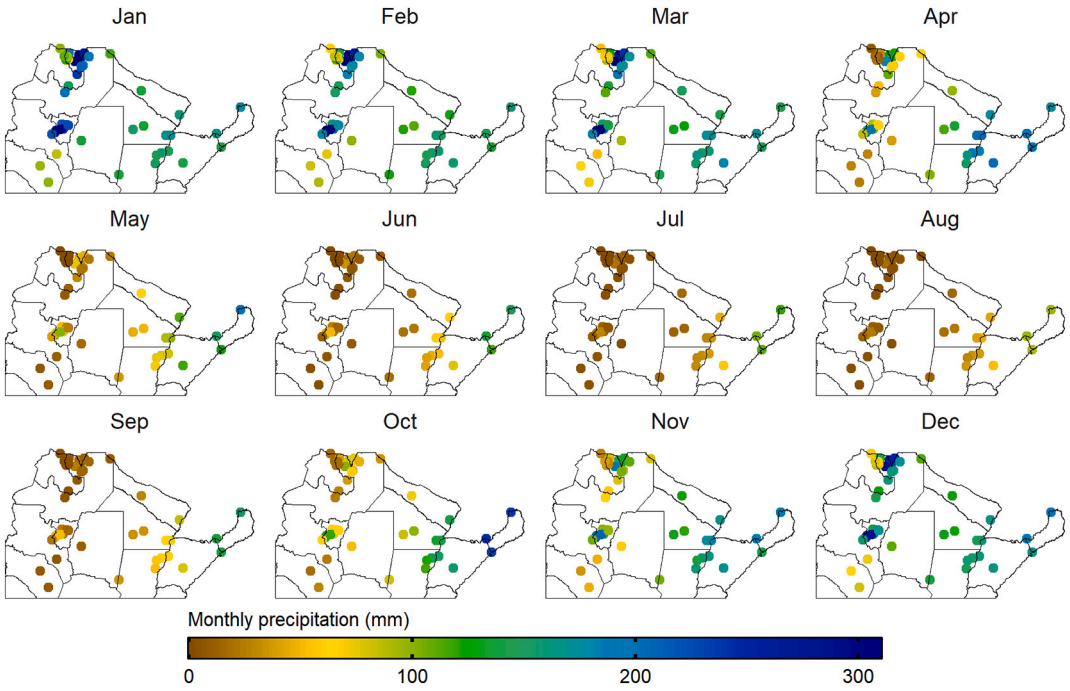

Fig. 3. Mean monthly precipitation in the 1990–2019 period for OBS data.

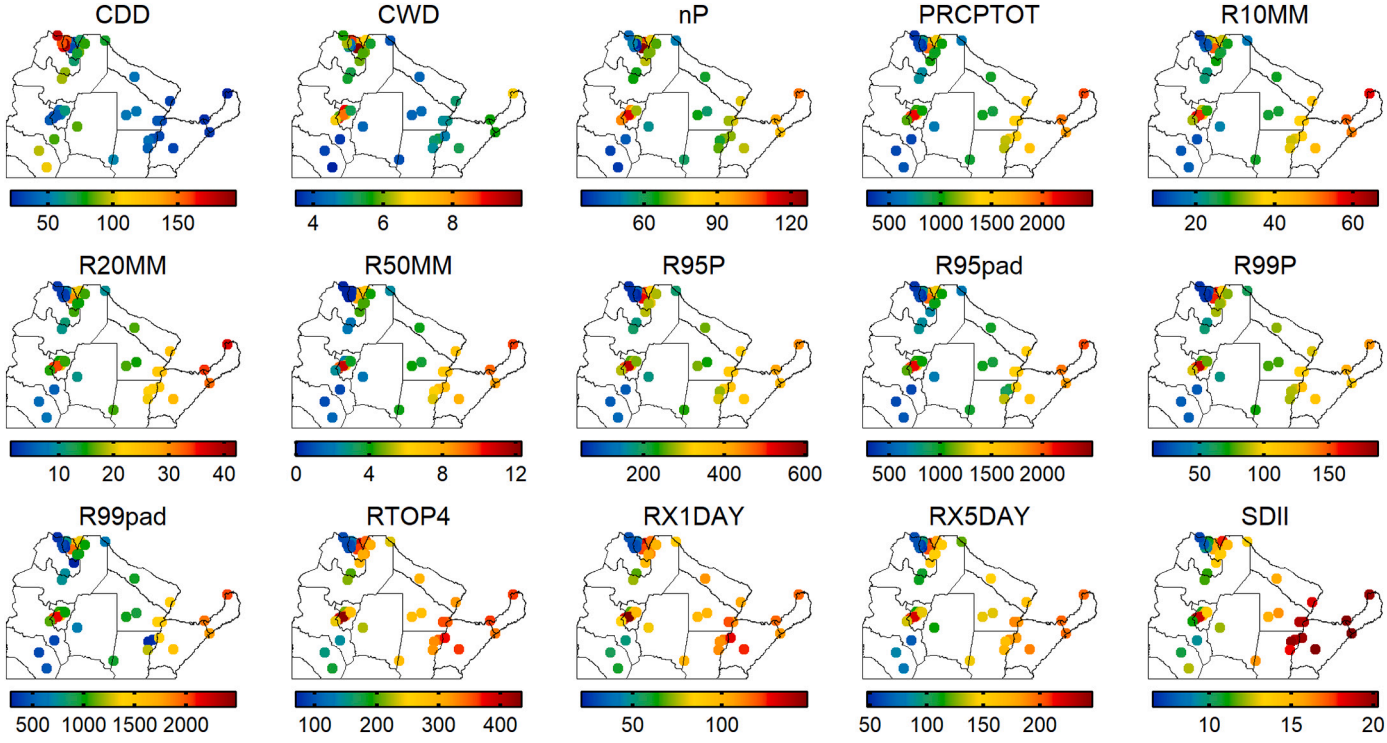

Fig. 4. Mean annual rainfall indices in the 1990–2019 period from OBS data.

equivalent to the sum of the 12 panels in Fig. 3. Stations in the west extreme have the lowest PRCPTOT, compatible with the highest CDD values observed at the same stations. In comparison, this drier zone has on average less than half of PRCPTOT (< 500 mm) and more than duplicate CDD values (>100 days) than the rest of NA. Two well defined zones with PRCPTOT maximum values can be noted: one at NWA center and the other in eastern NEA, consistent with the monthly analysis. For the other rainfall indices, except for CWD, the spatial pattern is similar to that of PRCPTOT with a stronger longitudinal than latitudinal gradient. In CWD case, maximum values are present in a great part of NWA with values up to 8 days. Discerning between anchor and no-anchor stations, as can be deduced from Fig. S2, NWA no-anchor stations present higher annual rainfall indices than anchor stations in most of the cases. In the case of NEA, similar to the monthly rainfall case (Fig. 2), no marked differences between anchor and no-anchor rainfall index values are observed.

4.2. Performance for monthly rainfall

Fig. 5 shows monthly rainfall values from CHIRPS versus the corresponding values from OBS distinguishing NWA and NEA regions, as well as anchor and no-anchor stations. Our results indicate that CHIRPS data strongly underestimate the highest monthly rainfall in no-anchor stations over NWA (Fig. 5, lower panel) as evinced by the blue dots well below the 1:1 line for the highest OBS data values. In the rest of the stations, at both NWA and NEA regions, even though in a lesser extent, an underestimation can also be observed for OBS values above ~400 mm noting that dots almost systematically fall below the 1:1 line.

The squared RHO values (displayed in each panel of Fig. 5) indicate that CHIRPS has the lowest performance representing rainfall values variability in the case of NWA no-anchor stations ($RHO^2 = 0.64$). In the rest of the cases, RHO^2 is higher than 0.70. It is worth noting that, as already mentioned, NWA no-anchor stations are located in NA zones of strong elevation gradients and with some of the highest rainfall values.

Curves of frequency density constructed with daily OBS and CHIRPS data are shown in Fig. 6. CHIRPS underestimates OBS frequency at the lowest and highest rainfall values in the cases of NEA anchor and no-anchor stations, and in the case of NWA anchor stations. That is, rainfall frequencies at NEA anchor (no-anchor) stations under 20 (15) mm and above 195 (190) mm are underestimated, while being overestimated between these values. In the similar case of NWA anchor stations, these limiting values are 5 mm and 200 mm. Regarding NWA no-anchor stations, frequency density of rainfall values under 30 mm and between 70 and 200 mm are overestimated, while for values between 30 mm and 70 mm and above 200 mm an underestimation is observed. The underestimation of higher rainfall frequency is expected as a result of the CHIRPS building-process that eliminates more extreme observed rainfall values (Funk et al., 2015), and also due to the disaggregation process from pentad to daily rainfall.

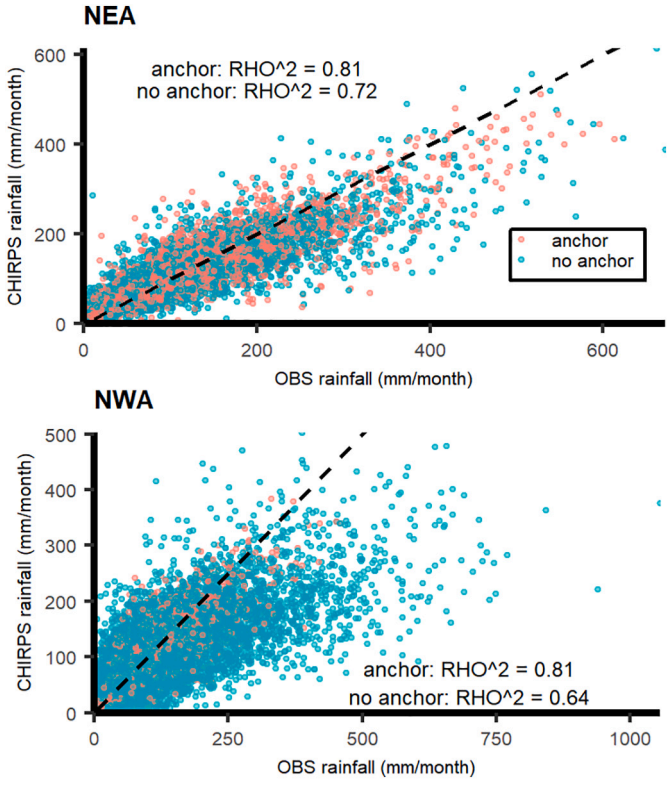

Fig. 5. Scatter plot of OBS and CHIRPS monthly rainfall for the 1982–2019 period for NWA (lower panel) and NEA (upper panel), for anchor (pink dots) and no-anchor (blue dots) stations. The dashed line indicates 1:1. (For interpretation of the references to colour in this figure legend, the reader is referred to the web version of this article.)

Regarding the four statistical metrics here analyzed, the spatial distribution of each one is shown in Figs. 7 to 10, and the corresponding frequency distributions in Figs. S3 to S6. In the case of RHO, shown in Fig. 7, overall lower values are observed in NWA than in NEA, especially for the driest months, with values even lower than 0.5 and a few which are statistically non-significant (see also Fig. S3). Within NEA, RHO is greater for the driest months (June to September) than for the rainiest (October to May). In NWA the inverse behavior is noticed, that is RHO is greater for the rainiest months (October to April) than for the driest (May to September). This can also be noticed from RHO frequency distribution curves (Fig. S3). In addition, in the case of NEA it can be clearly noticed that most RHO values are >0.5 for all months while in the case of NWA RHO decreases in some cases (especially in the no-anchor case) to values below significance. Fig. S3 also shows that NEA anchor and no-anchor stations behave more similarly between them than in the case of NWA. In the latter case RHO values and distribution for anchor stations are markedly different from those of no-anchor stations.

Fig. 8 shows MRE spatial distribution. As in the case of RHO, a better CHIRPS performance is detected for NEA than for NWA in all months (see also Fig. S4). In the case of NEA, for anchor and no-anchor stations, optimal MRE values (about zero) are noticed in wettest months ranging between −0.15 and + 0.15. In NWA the best performance is detected for anchor stations in February and March. In this region some isolated cases of a strong overestimation (red dots) can be noticed in April, May and June. The worst cases, with MRE values up to −1, occur for NWA driest months in most stations, and in almost every month in the case of no-anchor stations. In general, the frequency distribution (see Fig. S4) shows that CHIRPS underestimates monthly rainfall values in NA specially in no-anchor stations of NWA, while Fig. 8 evidence that the most MRE extreme values are observed over the center and the north-extreme of NWA where the no-anchor stations are located.

In the case of MAE, shown in Fig. 9, it is noticeably lower during the driest months, which is expected taking into account MAE's scale dependence and that the mean rainfall during these months is much lower than during the rainiest season. According to its spatial distribution, CHRIPS performs better in NEA than in NWA during the rainiest months (November to April), and in vice versa during the driest months (May to August). The maximum MAE is observed in the January month in one location of the center of NWA with a value of 247 mm.

NSE spatial variation, seen in Fig. 10, shows as in the case of RHO that CHIRPS has a better performance in NEA than in NWA, with values closer to 1 in most of NEA region, for anchor and no-anchor stations (see Fig. S6). Within NWA, CHIRPS anchor stations have better values of NSE than no-anchor where the NSE values are almost −2.5 in the worst case. From Fig. S6, almost all distribution curves, except some cases of NWA no-anchor stations, lie mainly between 1 and 0, indicating that the residual variance between CHIRPS and OBS are lower than the OBS variance in each case.

4.3. Performance for annual rainfall indices

The spatial distribution of each comparison statistical metric for the annual rainfall indices is shown in Figs. 11 to 14, and the corresponding histograms in Figs. S7 to S10. In the case of RHO values, shown in Fig. 11 (and Fig. S7), non-significant values can be noticed in many stations for some number-days based indices related with the 1 mm threshold (CDD, CWD, nP) and very extreme indices (for instance R99P, RX1DAY). In these cases, the better values of RHO are observed in anchor stations of NEA centered between 0.4 and 0.6 by the index. On the other hand, PRCPTOT, R95pad, R99pad, R10MM and R20MM are observed to have much higher RHO values in comparison with other indices, especially in the east of NEA. These high values correspond mainly to anchor stations (see Fig. S7) in both regions. For example, for NWA no-anchor stations, PRCPTOT, R95pad and R99pad present a RHO distribution centered in the lowest statistical significant value (indicated by a vertical dashed

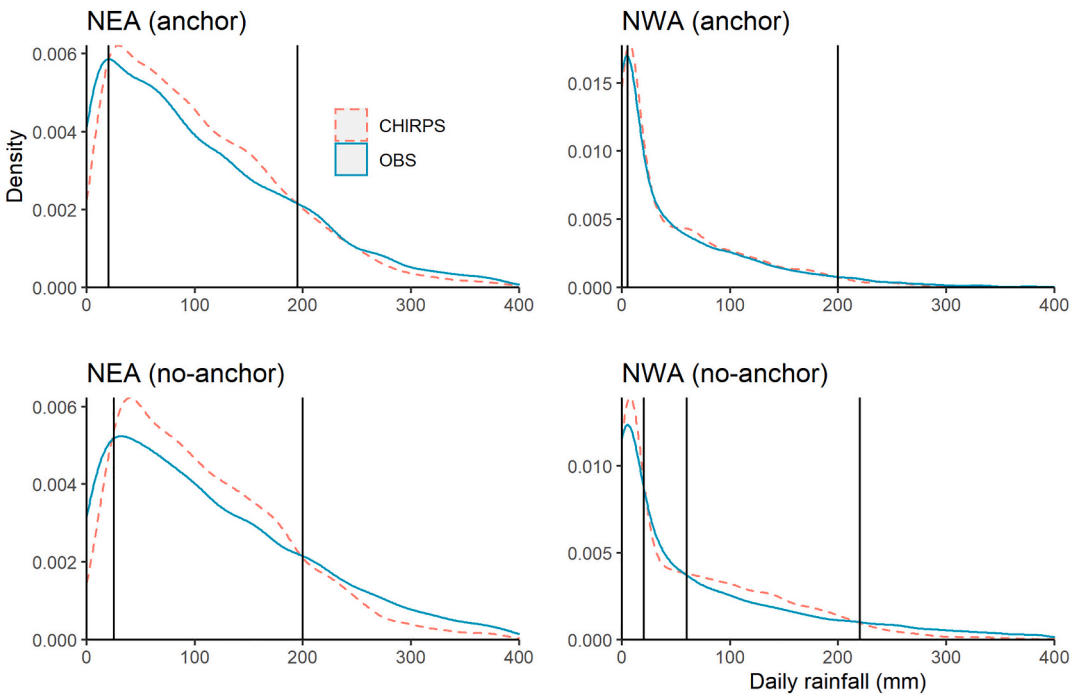

Fig. 6. Frequency density of daily rainfall for OBS (solid blue line) and CHIRPS (dashed pink line) for the 1982–2019 period for NEA (left panels) and NWA (right panels), for anchor (upper panels) and no-anchor (lower panels) stations. Vertical lines indicate rainfall values where there is a change in the position (above or below) of CHIRPS curve with respect of OBS curve. (For interpretation of the references to colour in this figure legend, the reader is referred to the web version of this article.)

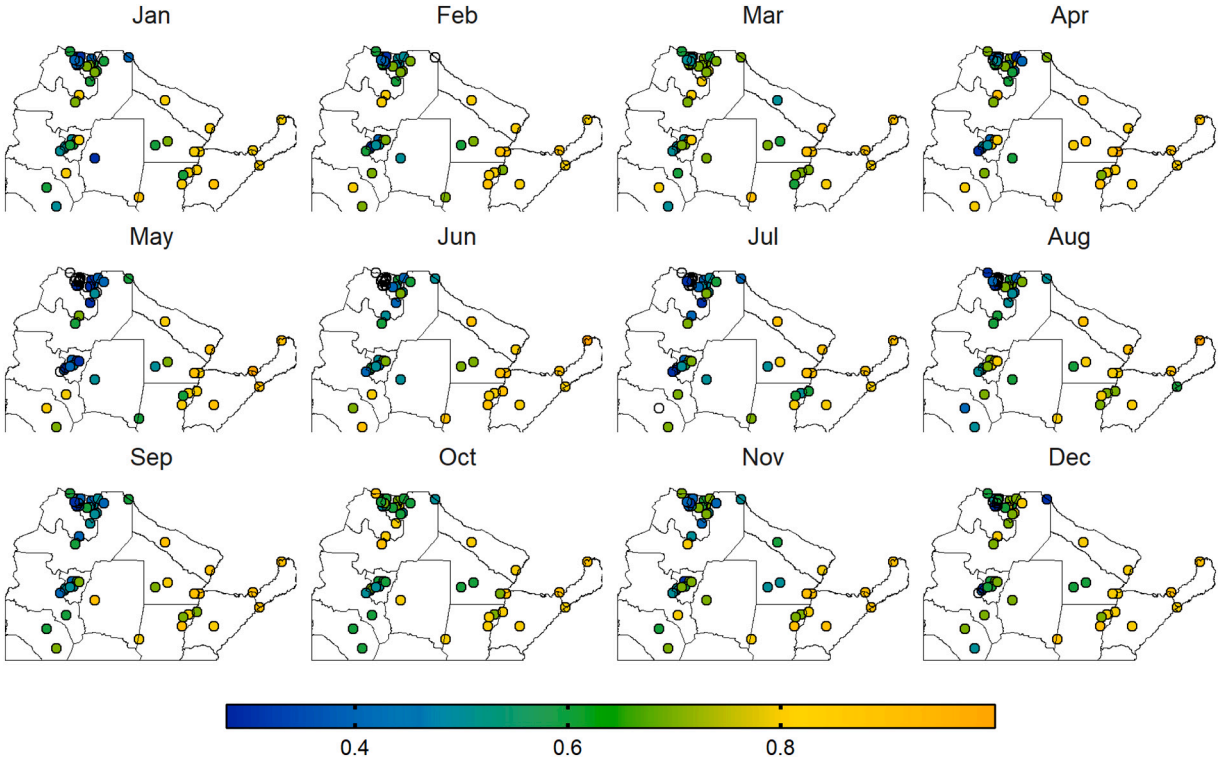

Fig. 7. Spatial distribution of RHO values between OBS and CHIRPS monthly rainfall for the 1982–2019 period. Non-significant RHO values appear as empty circles.

black line in Fig. S7) while for anchor stations it is centered in ~0.7.

In the cases of PRCPTOT, R95pad and R99pad, MRE values close to zero in most of the stations is added to the good correlation already observed, as can be seen in Fig. 12. In addition, in Fig. S8 it can be noticed that these three indices for anchor stations in the whole NA region have the sharpest distribution around zero. However, CHIRPS overall underestimate most of the indices in most of the stations. The greatest underestimation corresponds to R50MM, followed by Rx1DAY, RTOP4, R99P and R95P, which are very-extreme indices that can be more sensitive and therefore have great relative bias when gauge-

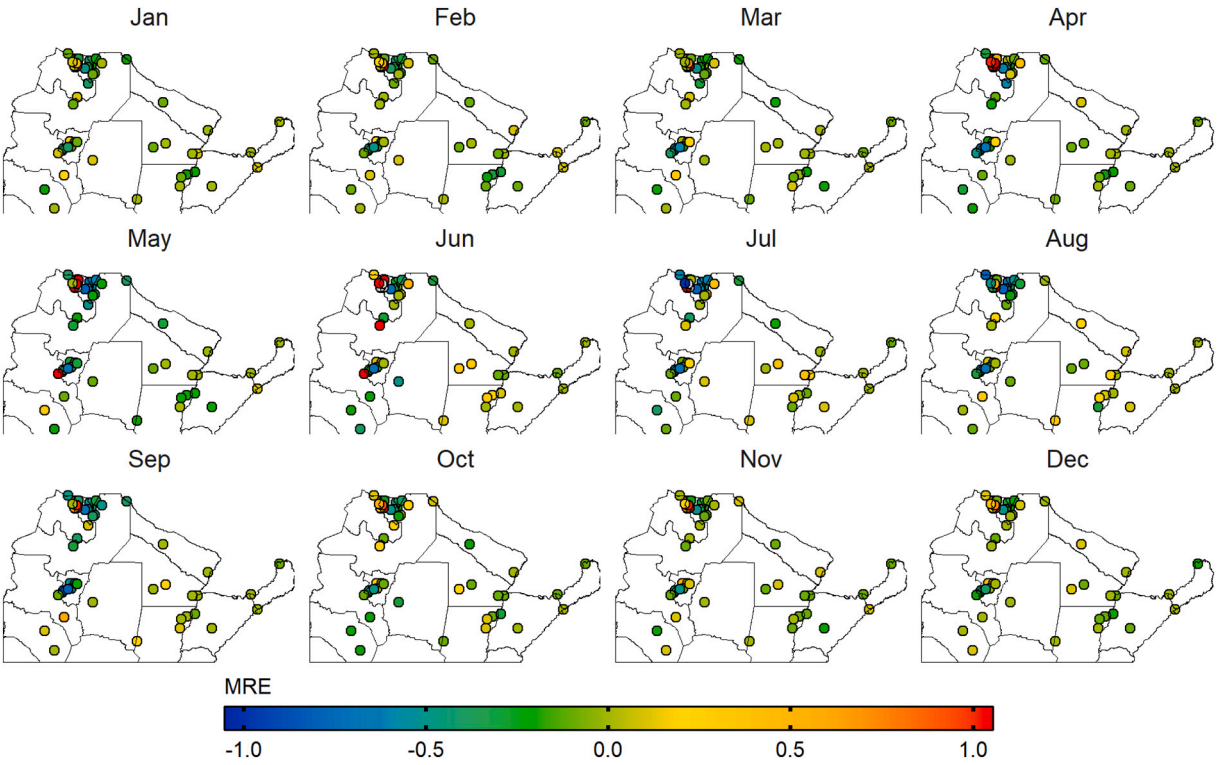

Fig. 8. Spatial distribution of monthly MRE values between OBS and CHIRPS monthly rainfall for the 1982–2019 period.

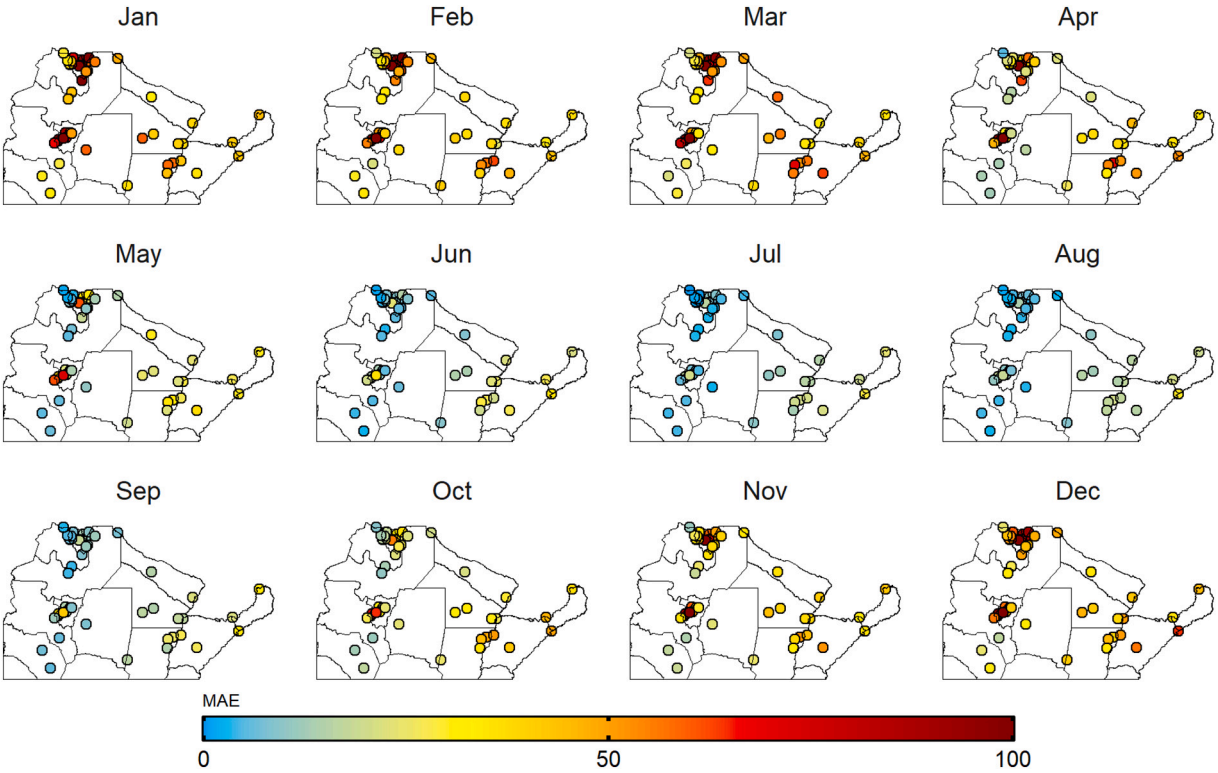

Fig. 9. Spatial distribution of monthly MAE values between OBS and CHIRPS monthly rainfall for the 1982–2019 period.

stations are not used in CHIRPS production, especially in zones with great rainfall gradients as NWA.

In the case of MAE (see Fig. 13 and Fig. S9), CHIRPS better represents NEA in the case of CDD, CWD, nP and SDII. In the remaining cases, NWA is better represented in the particular case of anchor stations. For no-anchor stations MAE values are more spread towards higher values in both regions, as can be noticed in Fig. S9. Consistent with MRE, PRCPTOT, R95pad and R99pad have the sharpest distributions closest to

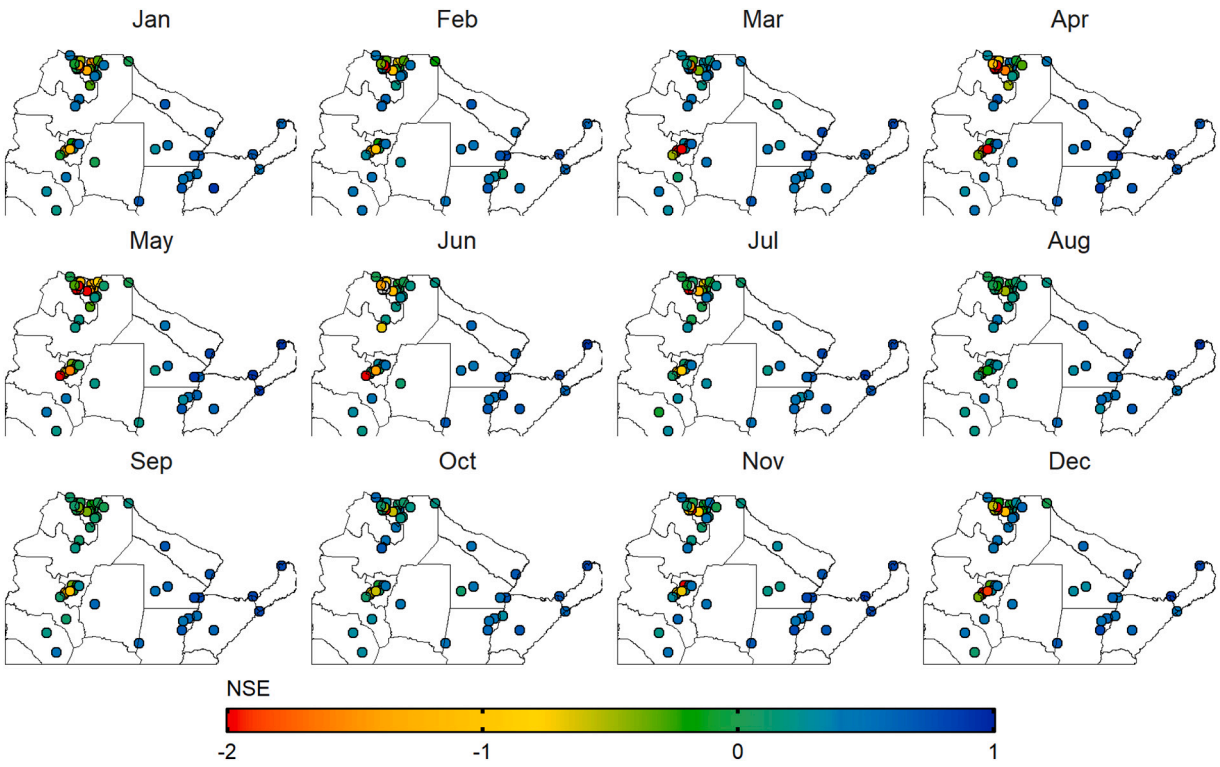

Fig. 10. Spatial distribution of monthly NSE values between OBS and CHIRPS monthly rainfall for the 1982–2019 period.

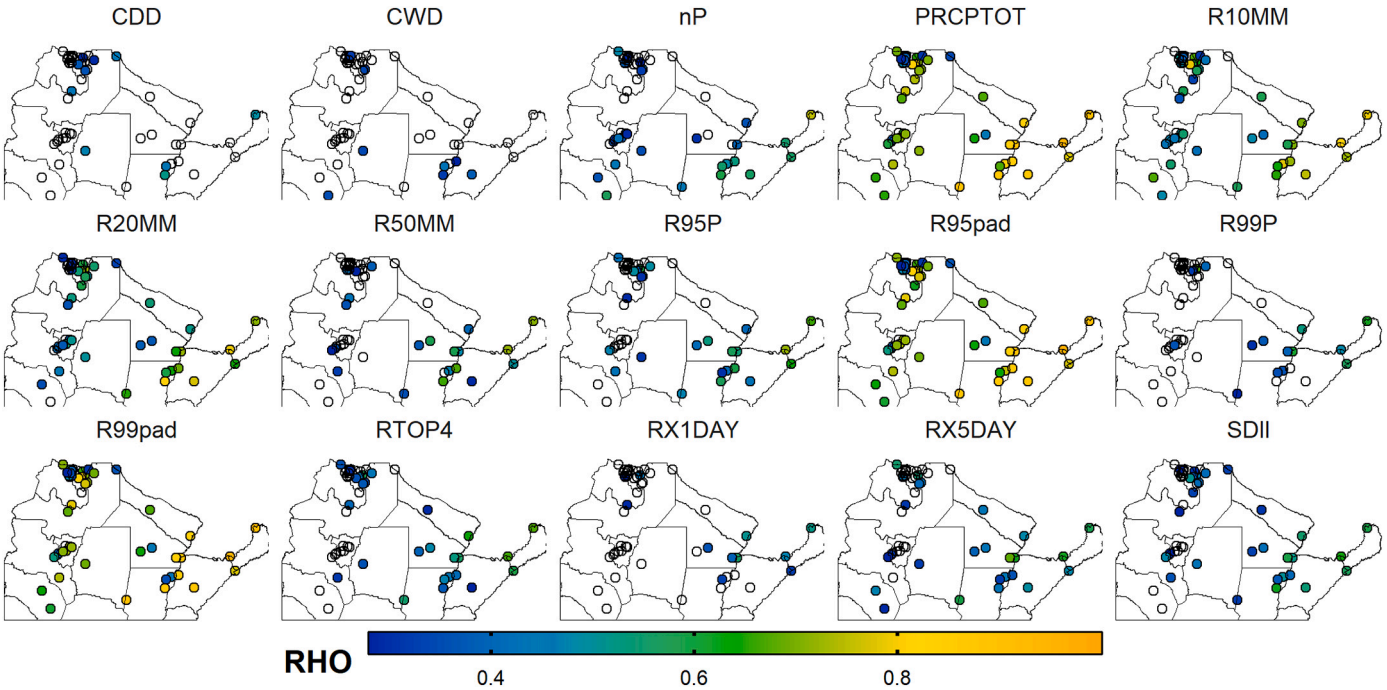

Fig. 11. Spatial distribution of RHO values between OBS and CHIRPS annual rainfall indices for the 1982–2019 period. Non-significant RHO values appear as empty circles.

zero in the case of anchor stations for both regions, NWA and NEA (see Fig. S9).

In the case of NSE, shown in Fig. 14, PRCPTOT, R95pad and R99pad present overall the optimum values, and in particular for NEA anchor stations (see Fig. S10) where the maximum value observed is 0.88 for PRCPTOT in comparison with values under −1 in some no-anchor stations of NWA. For the other indices, in general variance between CHIRPS and OBS exceeds the OBS variance (NSE < 0).

4.4. *Performance for linear trends in rainfall indices*

The location of stations shown in Fig. 15, indicate if the corresponding rainfall index trend is significant in the case of CHIRPS, of OBS, of both simultaneously or in neither of them. Their values can be seen in

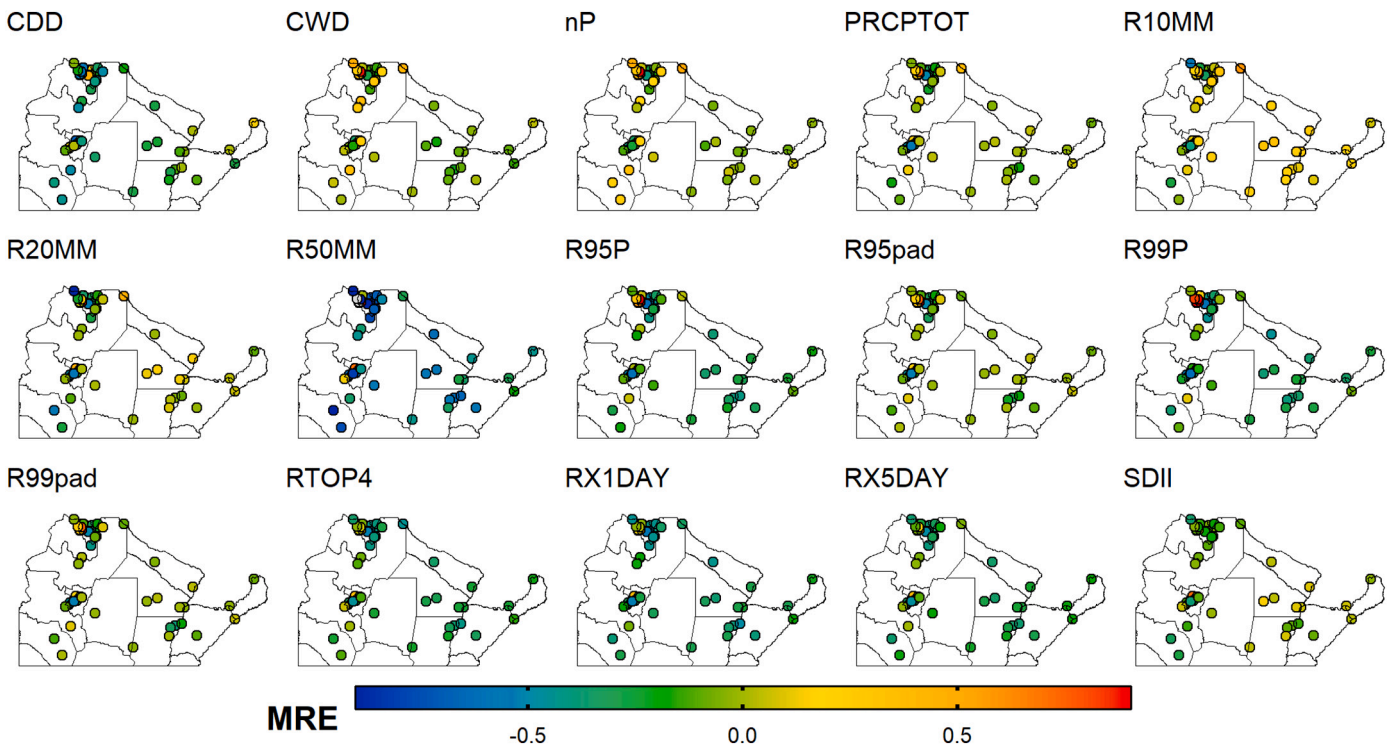

Fig. 12. Spatial distribution of MRE values between OBS and CHIRPS annual rainfall indices for the 1982–2019 period.

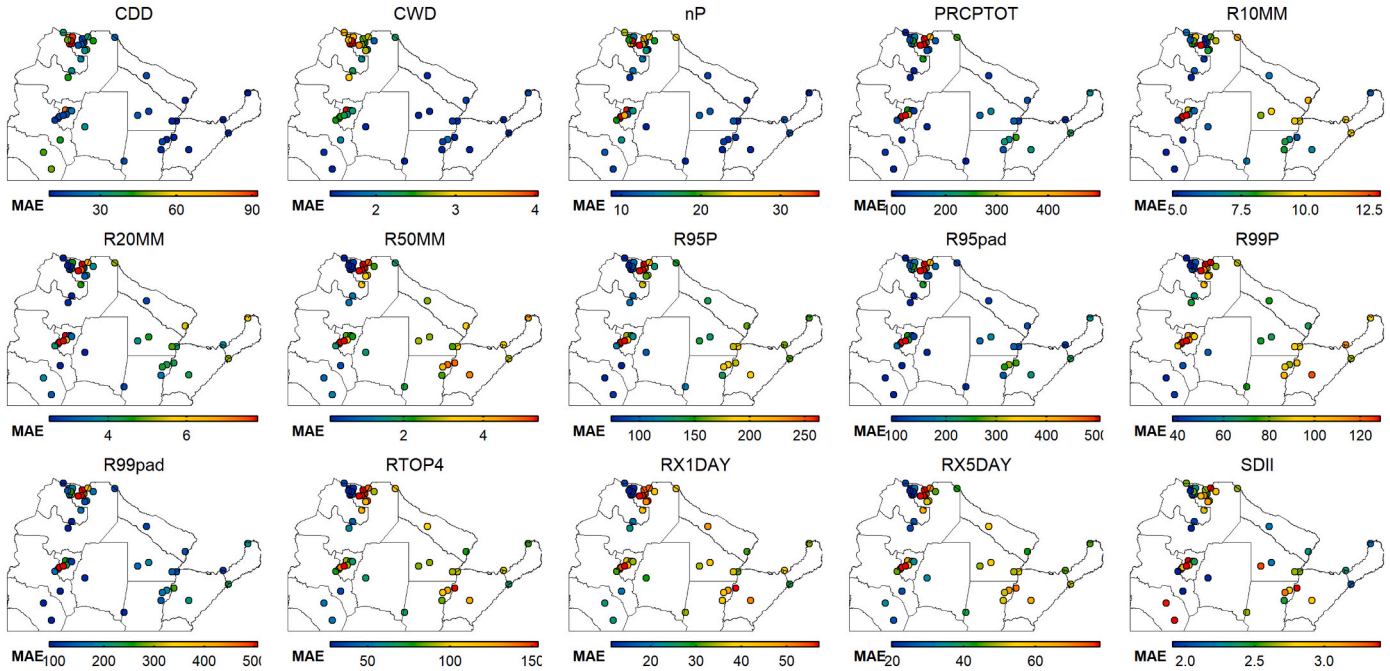

Fig. 13. Spatial distribution of MAE values between OBS and CHIRPS annual rainfall indices for the 1982–2019 period.

the dispersion diagram in Fig. S11 showing CHIRPS vs. OBS trends. There are only two trends out of ninety in OBS that are detected simultaneously in CHIRPS: a positive trend in CDD, similar in both cases, and a negative trend in R99P, stronger in OBS than in CHIRPS, at the same NWA anchor station. In the case of CDD, even though there is only one coincidence, it is worth noting that both, CHIRPS and OBS, detect positive trends concentrated in northern NWA. However, a lack of CHIRPS ability for trend detection in rainfall indices is noted overall, with more trends detected in OBS than in CHIRPS. The undetected trends occur both for anchor and no-anchor stations, being fifteen for anchor and seventy-three for no-anchor stations, with nP the index with more trends OBS which are undetected in CHIRPS.

CHIRPS detect negative trends in RX1DAY, R99P and RTOP4 at NEA stations which are not detected with OBS. However, in the cases of RX1DAY and RTOP4 many of these trends have similar values to OBS trends despite the lack of significance in the latter case.

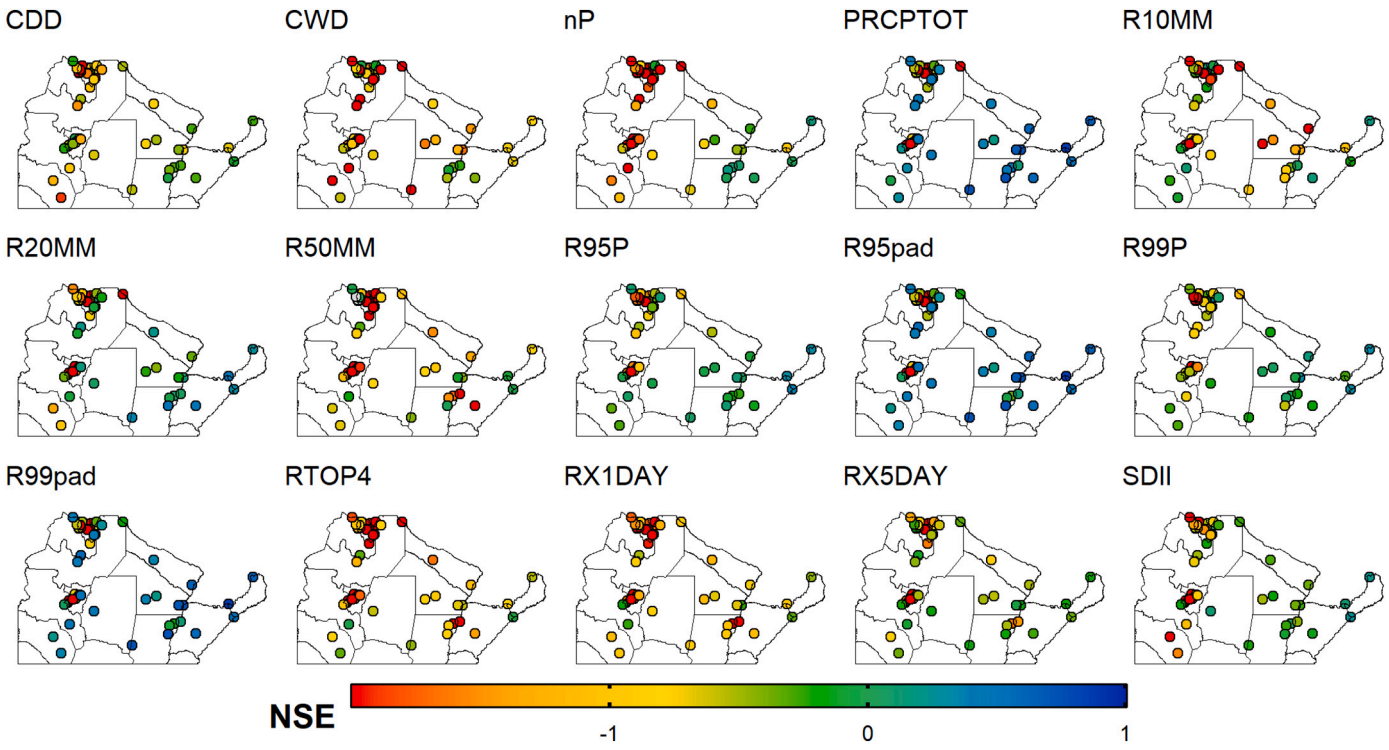

Fig. 14. Spatial distribution of NSE values between annual rainfall indices from OBS and CHIRPS data for the 1982–2019 period.

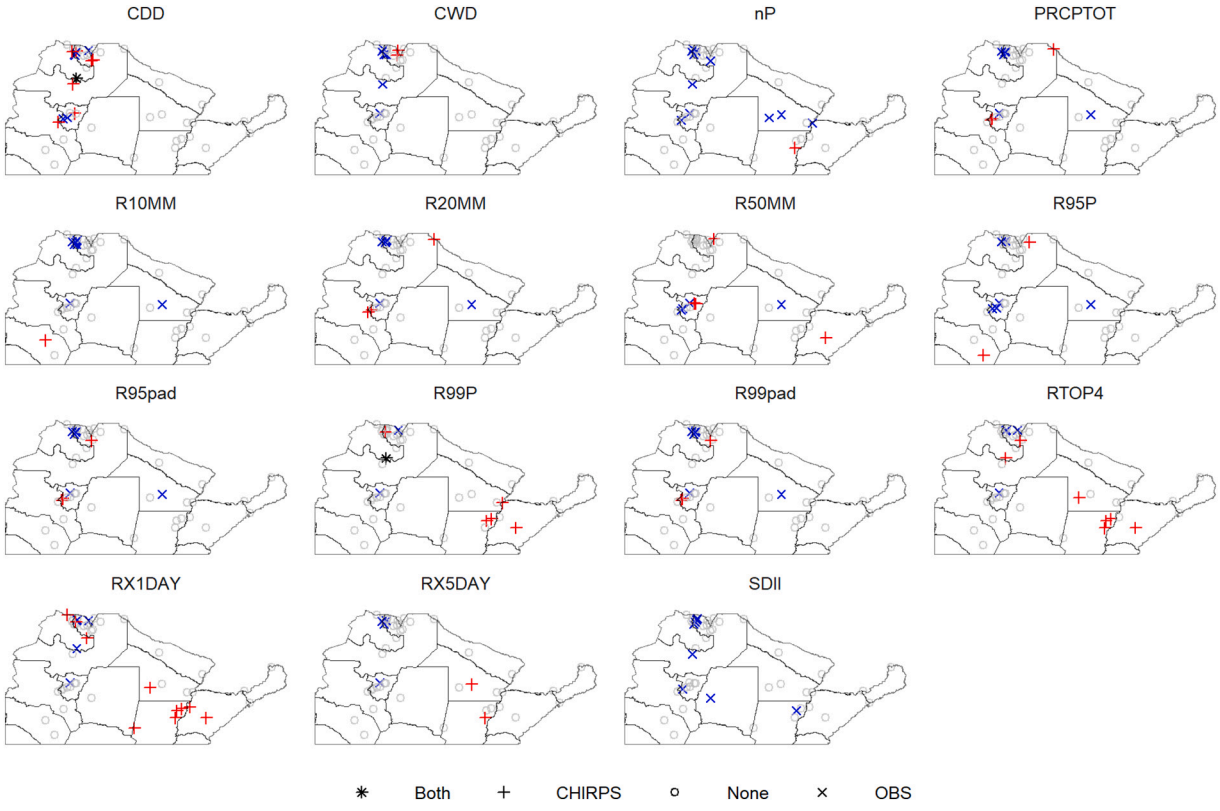

Fig. 15. Location of the stations with significant trends ($p < 0.05$) detected for OBS (blue cross), CHIRPS (red plus) and both data series (black asterisk) for annual rainfall indices along the 1982–2019 period. Gray circles indicate stations with no significant trend. (See Fig. S11 for the trends' sign and values). (For interpretation of the references to colour in this figure legend, the reader is referred to the web version of this article.)

5. Discussion and conclusions

The underestimation of rain gauge data by CHIRPS in the case of high rainfall values determined in this work for NA, is in agreement with the result obtained by Cavalcante et al. (2020) for BLA. In our case, having distinguished between anchor and no-anchor stations, we have detected that this occurs particularly for no-anchor stations (especially in NWA) as can be noticed in Fig. 5. Regarding frequency distribution, also in coincidence with Cavalcante et al. (2020), CHIRPS overall underestimates low and high rainfall values' frequency in comparison to OBS. In our case this occurs in NEA for all stations and in NWA for anchor stations.

The lower RHO values in NWA with respect to NEA in all months agrees with previous results about the lower performance of CHIRPS in mountain regions (Funk et al., 2015; Gupta et al., 2019) where rainfall spatial variability is strong and smaller scale. In addition, the lower RHO values for drier climatic conditions obtained in NWA is a common characteristic observed in CHIRPS and similar products in others regions of the world (Liu et al., 2019; Zhang et al., 2022), due to their lower detection ability for lighter rainfall. This result agrees with results for the north of Chile (country bordering east of Argentina) where the precipitation estimates from CHIRPS were more accurate from December to March when higher rainfall amounts occur (Zambrano et al., 2017), with both regions having marked rainfall annual cycles. In contrast, in NEA the greatest RHO values were verified in driest months in agreement with results for the Amazon region obtained by de Moraes Cordeiro and Blanco (2021). In NEA the rainfall decrease is weaker and thus detection ability can be better. The Amazon region provides humidity flux to the NEA region sustained along the whole year (Vera et al., 2002), and thus, similar results are expected due to the connection between rainfall in these regions. In wetter months, strong convection and cloud cover non-related with rainfall are present, with a consequent increase of the erroneous detection of rainfall from satellite estimation. In driest months this effect is reduced and rainfall is better represented. However, in NWA and north of Chile rainfall values drop strongly in the dry season and the detection of the few and lighter rainfall episodes, as already mentioned, is more difficult.

A comparison can be made of our monthly rainfall analysis in NA with that of Cerón et al. (2020) in La Plata Basin, since the latter includes NEA and much of NWA. Rainfall series in Cerón et al. (2020) case consists of monthly means but without separating them into each month, so their time series have the seasonal variation included while ours do not. We consider that this fact improves RHO performance in their case, since both series, CHIIRPS and OBS have the seasonal variation which is stronger and more likely to resemble than the interannual variation. Turning now to MRE, equivalent to the bias in Cerón et al. (2020), considering an average of monthly MRE (Fig. 8) in our case, there is an agreement in the NEA region with the lowest values and thus the best CHIRPS performance. Also in the NWA region, CHIRPS main underestimation with some isolated MRE positive values in the center and northern extreme of NWA agrees in both studies. In the case of MAE, it is similar, even though not equal, to RMSE used by Cerón et al. (2020). Considering again that their analysis includes all the months as single time series, they obtain a range between 40 and 90 mm, which is a little lower than ours. Circumscribing their results for NA, the highest values are seen in eastern NEA, as in our case during winter (the driest months), and also in the central area of NWA as in our case during summer (the rainiest months). We have some isolated MAE values reaching 100 mm and more.

Going to rainfall indices, for the very extreme ones, the literature has similar results concerning a lower performance of CHIRPS as in Cavalcante et al. (2020) and Paredes Trejo et al. (2016). With respect to the low performance in the case of indices related to number days, Katsanos et al. (2016) attribute it to a deficiency in the criteria used for the identification of a wet day. In addition, Paredes Trejo et al. (2016) point out the low capabilities of CHIRPS for detection of rainfall events. Indices based on number days are affected directly by these deficiencies, while very extreme indices are affected too because they are related to one or a few daily events. In particular, based on the four statistics used in this study, the more similar results between CHIRPS and OBS in the cases of PRCPTOT, nP and R95pad obtained by Cavalcante et al. (2020) for BLA, together with the strong underestimation they observe in the most extreme rainfall indices (R50mm, Rx1day, Rx5days) is also obtained in this study for NA, even though not for the whole region.

Moving to trend results, the deficiencies detected here for trend analysis using CHIRPS are in agreement with similar studies in other regions of the world such as India and Brazil (Cavalcante et al., 2020; Bhattacharyya et al., 2022). However, it should be mentioned that there are regions of the world, such as sub-Saharan Africa or Pakistan, where CHIRPS is among the best to analyze long-term changes in extreme rainfall (Harrison et al., 2019; Nawaz et al., 2021). Our study, where anchor and no-anchor stations were distinguished, allowed us to identify the existence of undetected trends both in anchor and no-anchor stations, and thus, we can conclude that the incorporation of stations in the CHIRPS production does not necessarily guarantee the linear trend representation.

In the case of CDD trends, our results are in agreement with the increase in this same region, reported by Skansi et al. (2013) for the period 1969–2009, and Balmaceda Huarte et al. (2021) for the period 1979–2017. So, we can conclude that CDD presents a sustained increasing trend since 1969 at least. It could also be said that CHIRPS have problems to detect accurately locations of significant CDD trends (Fig. 15). However, increasing to a regional scale, the detection improves.

Summarizing, a validation of CHIRPS rainfall dataset was performed for NA, distinguishing two separate regions: NWA and NEA, and also anchor and no-anchor rain gauge stations. This validation was done using daily data covering a period of 38 years (1982–2019) and 50 stations, not used before for this purpose. Concerning monthly rainfall, CHIRPS dataset better represents the interannual variability of monthly rainfall in wetter (drier) months in NWA (NEA). However, regarding intensity, CHIRPS underestimates NA monthly values, with the most extreme MRE negative values observed over the center of NWA, during the rainiest months, where the no-anchor stations are located.

About the temporal variability of rainfall indices, RHO values in most of the stations of NA are non-significant for some number-days based indices related with the threshold of 1 mm (CDD, CWD, nP) and very extreme indices (R99P, RX1DAY, R50MM). Only a few stations of eastern NA have significant RHO values for these indices. The less extreme indices PRCPTOT, R95pad, R10MM and R20MM are observed to have higher RHO values in both regions without differences between anchor and no-anchor stations. From MRE values, it can be concluded that CHIRPS underestimate most of the indices in most of the stations. This is more evident in no-anchor stations of NWA for total-accumulated and very-extreme indices due to the higher spatial variability along this region.

Concerning long-term trends, most of the significant linear trends observed in rainfall indices are not detected with CHIRPS. As an exception, a relatively better performance for CDD is observed in the sense that CHIRPS detect the positive linear trends in NWA but do not locate them with precision. This relatively better performance for CDD is related with the recommendation of the use of CHIRPS for drought monitoring, but performance in NA still must improve.

As a recommendation, and in coincidence with Cavalcante et al. (2020) we consider that CHIRPS is not indicated for studies in NA related with the aspects (mean values, interannual variability, linear trends) of rainfall analyzed in this work, especially for the extreme rainfall. The inclusion in the CHIRPS production of no-anchor stations, can highly enhance their representation.

CRediT authorship contribution statement

Franco D. Medina: Conceptualization, Methodology, Data curation, Software, Validation, Formal analysis, Writing – original draft, Writing – review & editing. **Bruno S. Zossi:** Conceptualization, Software, Writing – review & editing. **Adriana Bossolasco:** Conceptualization, Software, Writing – review & editing. **Ana G. Elias:** Conceptualization, Supervision, Writing – review & editing.

Declaration of Competing Interest

The authors declare that they have no known competing financial interests or personal relationships that could have appeared to influence the work reported in this paper.

Data availability

Data will be made available on request.

Acknowledgements

The authors acknowledge CONICET Research Project PIP 2957.

Appendix A. Supplementary data

Supplementary data to this article can be found online at https://doi.org/10.1016/j.atmosres.2022.106545.

References

Baez-Villanueva, O.M., Zambrano-Bigiarini, M., Ribbe, L., Nauditt, A., Giraldo-Osorio, J. D., Xuan, N., Thinh, N.X., 2018. Temporal and spatial evaluation of satellite rainfall estimates over different regions in Latin-America. Atmos. Res. 213, 34–50. https://doi.org/10.1016/j.atmosres.2018.05.011.

Balmaceda Huarte, R., Olmo, M.E., Bettolli, M.L., Poggi, M.M., 2021. Evaluation of multiple reanalyses in reproducing the spatio-temporal variability of temperature and precipitation indices over southern South America. Int. J. Climatol. 41, 5572–5595. https://doi.org/10.1002/joc.7142.

Barreiro, M., Díaz, N., Renom, M., 2014. Role of the global oceans and land–atmosphere interaction on summertime interdecadal variability over northern Argentina. Clim. Dyn. 42 (7), 1733–1753. https://doi.org/10.1007/s00382-014-2088-6.

Barros, V., Doyle, M., Camilloni, I., 2008. Precipitation trends in southeastern South America: relationship with ENSO phases and with low-level circulation. Theor. Appl. Climatol. 93, 19–33. https://doi.org/10.1007/s00704-007-0329-x.

Bello, O.D., Ballesteros, J., Buitrago, M., González, M., Velasco, O., 2018. Análisis Retrospectivo de Las Inundaciones: Lecciones Y Recomendaciones - Argentina, Documento de Proyecto. Publicación de las Naciones Unidas y CEPAL. https://www.cepal.org/sites/default/files/static/files/lcarts2018_1-final.pdf.

Bhattacharyya, S., Sreekesh, S., King, A., 2022. Characteristics of extreme rainfall in different gridded datasets over India during 1983–2015. Atmos. Res. 267, 105930 https://doi.org/10.1016/j.atmosres.2021.105930.

Bookhagen, B., Strecker, M.R., 2008. Orographic barriers, high-resolution TRMM rainfall, and relief variations along the eastern Andes. Geophys. Res. Lett. 35, L06403. https://doi.org/10.1029/2007GL032011.

Carvalho, L.M.V., 2020. Assessing precipitation trends in the Americas with historical data: a review. WIREs Clim. Change. 2020 (11), e627 https://doi.org/10.1002/wcc.627.

Castino, F., Bookhagen, B., Strecker, M.R., 2017. Rainfall variability and trends of the past six decades (1950–2014) in the subtropical NW Argentine Andes. Clim. Dyn. 48 (3), 1049–1067. https://doi.org/10.1007/s00382-016-3127-2.

Cavalcante, R.B.L., da Silva Ferreira, D.B., Pontes, P.R.M., Tedeschi, R.G., da Costa, C.P. W., de Souza, E.B., 2020. Evaluation of extreme rainfall indices from CHIRPS precipitation estimates over the Brazilian Amazonia. Atmos. Res. 238, 104879 https://doi.org/10.1016/j.atmosres.2020.104879.

Cerón, W.L., Molina-Carpio, J., Ayes Rivera, I., et al., 2020. A principal component analysis approach to assess CHIRPS precipitation dataset for the study of climate variability of the La Plata Basin, Southern South America. Nat. Hazards 103, 767–783. https://doi.org/10.1007/s11069-020-04011-x.

Cerón, W.L., Kayano, M.T., Andreoli, R.V., Avila-Diaz, A., Ayes, I., Freitas, E.D., Martins, J.A., Souza, R.A.F., 2021. Recent intensification of extreme precipitation events in the La Plata Basin in Southern South America (1981–2018). Atmos. Res. 249, 105299. ISSN 0169-8095. https://doi.org/10.1016/j.atmosres.2020.105299.

de Moraes Cordeiro, A.L., Blanco, C.J.C., 2021. Assessment of satellite products for filling rainfall data gaps in the Amazon region. Nat. Resour. Model. 34, e12298 https://doi.org/10.1111/nrm.12298.

Doyle, M.E., 2020. Observed and simulated changes in precipitation seasonality in Argentina. Int. J. Climatol. 2020 (40), 1716–1737. https://doi.org/10.1002/joc.6297.

Faiz, M.A., Liu, D., Fu, Q., Sun, Q., Li, M., Baig, F., Li, T., Cui, S., 2018. How accurate are the performances of gridded precipitation data products over Northeast China? Atmos. Res. 211, 12–20. https://doi.org/10.1016/j.atmosres.2018.05.006.

Ferrero, M.E., Villalba, R., 2019. Interannual and long-term precipitation variability along the subtropical mountains and adjacent Chaco (22–29° S) in Argentina. Front. Earth Sci. 7, 148. https://doi.org/10.3389/feart.2019.00148.

Fowler, H.J., Lenderink, G., Prein, A.F., et al., 2021. Anthropogenic intensification of short-duration rainfall extremes. Nat. Rev. Earth Environ. 2, 107–122. https://doi.org/10.1038/s43017-020-00128-6.

Funk, C., Peterson, P., Landsfeld, M., et al., 2015. The climate hazards infrared precipitation with stations—a new environmental record for monitoring extremes. Sci. Data 2, 150066. https://doi.org/10.1038/sdata.2015.66.

Gupta, V., Jain, M.K., Singh, P.K., Singh, V., 2019. An assessment of global satellite-based precipitation datasets in capturing precipitation extremes: a comparison with observed precipitation dataset in India. Int. J. Climatol. https://doi.org/10.1002/joc.6419.

Hamed, K.H., Rao, A.R., 1998. A modified Mann-Kendall trend test for autocorrelated data. J. Hydrol. 204 (1–4), 182–196. https://doi.org/10.1016/S0022-1694(97)00125-X.

Harrison, L., Funk, C., Peterson, P., 2019. Identifying changing precipitation extremes in Sub-Saharan Africa with gauge and satellite products. Environ. Res. Lett. 14, 085007 https://doi.org/10.1088/1748-9326/ab2cae.

Karl, T.R., Nicholls, N., Ghazi, A., 1999. Clivar/GCOS/WMO workshop on indices and indicators for climate extremes workshop summary. In: Weather and Climate Extremes. Springer, Dordrecht, pp. 3–7. https://doi.org/10.1007/978-94-015-9265-9_2.

Katsanos, D., Retalis, A., Tymvios, F., et al., 2016. Analysis of precipitation extremes based on satellite (CHIRPS) and in situ dataset over Cyprus. Nat. Hazards 83, 53–63. https://doi.org/10.1007/s11069-016-2335-8.

Kendall, M.G., 1955. Rank Correlation Methods. Griffin, London.

Laing, A.G., Fritch, J.M., 2000. The large-scale environments of the global populations of mesoscale convective complexes. Mon. Weather Rev. 128, 2756–2776. https://doi.org/10.1175/1520-0493(2000)128<2756:TLSEOT>2.0.CO;2.

Liu, J., Shangguan, D., Liu, S., Ding, Y., Wang, S., Wang, X., 2019. Evaluation and comparison of CHIRPS and MSWEP daily-precipitation products in the Qinghai-Tibet Plateau during the period of 1981–2015. Atmos. Res. 230, 104634. ISSN 0169-8095. https://doi.org/10.1016/j.atmosres.2019.104634.

Llano, M.P., 2018. Spatial distribution of the daily rainfall concentration index in Argentina: comparison with other countries. Theor. Appl. Climatol. 133, 997–1007. https://doi.org/10.1007/s00704-017-2236-0.

Lovino, M.A., Müller, O.V., Berbery, E.H., Müller, G.V., 2018. How have daily climate extremes changed in the recent past over northeastern Argentina? Glob. Planet. Chang. 168, 78–97. https://doi.org/10.1016/j.gloplacha.2018.06.008.

Mann, H.B., 1945. Nonparametric tests against trend. Econometrica 13. https://doi.org/10.2307/1907187.

Marengo, J.A., Liebmann, B., Grimm, A.M., Misra, V., Silva Dias, P.L., Cavalcanti, I.F.A., Carvalho, L.M.V., Berbery, E.H., Ambrizzi, T., Vera, C.S., Saulo, A.C., Nogues-Paegle, J., Zipser, E., Seth, A., Alves, L.M., 2012. Recent developments on the south American monsoon system. Int. J. Climatol. 32, 1–21. https://doi.org/10.1002/joc.2254.

Nash, J., Sutcliffe, J., 1970. River flow forecasting through conceptual models part I — A discussion of principles. J. Hydrol. 10 (3), 282–290. https://doi.org/10.1016/0022-1694(70)90255-6.

Nawaz, M., Iqbal, M.F., Mahmood, I., 2021. Validation of CHIRPS satellite-based precipitation dataset over Pakistan. Atmos. Res. 248 https://doi.org/10.1016/j.atmosres.2020.105289.

Paredes Trejo, F.J., Alves Barbosa, H., Peñaloza-Murillo, M.A., Moreno, M.A., Farías, A., 2016. Intercomparison of improved satellite rainfall estimation with CHIRPS gridded product and rain gauge data over Venezuela. Atmósfera 29 (4), 323–342.

Rivera, J.A., Marianetti, G., Hinrichs, S., 2018. Validation of CHIRPS precipitation dataset along the Central Andes of Argentina. Atmos. Res. 213, 437–449. ISSN 0169-8095. https://doi.org/10.1016/j.atmosres.2018.06.023.

Rivera, J.A., Hinrichs, S., Marianetti, G., 2019. Using CHIRPS Dataset to Assess Wet and Dry Conditions along the Semiarid Central-Western Argentina. Adv. Meteorol. https://doi.org/10.1155/2019/8413964.

Sen, P.K., 1968. Estimates of the regression coefficient based on Kendall's Tau. J. Am. Stat. Assoc. 63 https://doi.org/10.1080/01621459.1968.10480934.

Shrestha, D., Sharma, S., Hamal, K., Jadoon, U.K., Dawadi, B., 2021. Spatial distribution of extreme precipitation events and its trend in Nepal. Appl. Ecol. Environ. Sci. 9 (1), 58–66. http://pubs.sciepub.com/aees/9/1/8.

Skansi, M., Brunet, M., Sigró, J., Aguilar, E., Arevalo, J.A.G., Bentancur, O.J., et al., 2013. Warming and wetting signals emerging from analysis of changes in climate extreme indices over South America. Global Planet. Change 100 (2013), 295–307. ISSN 0921-8181. https://doi.org/10.1016/j.gloplacha.2012.11.004.

Sun, Q., Miao, C., Duan, Q., Ashouri, H., Sorooshian, S., Hsu, K.-L., 2018. A review of global precipitation data sets: data sources, estimation, and intercomparisons. Rev. Geophys. 56, 79–107. https://doi.org/10.1002/2017RG000574.

Vera, C., Vigliarolo, P.K., Berbery, E.H., 2002. Cold season synoptic scale waves over subtropical South America. Mon. Weather Rev. 130, 684–699. https://doi.org/10.1175/1520-0493(2002)130<0684:CSSSWO>2.0.CO;2.

Vera, C., Baez, J., Douglas, M., Emmanuel, C.B., Marengo, J., Meitin, J., Nicolini, M., et al., 2006. The South American low-level jet experiment. Bull. Am. Meteorol. Soc. 87 (1), 63–78. https://doi.org/10.1175/BAMS-87-1-63.

World Meteorological Organization (WMO), 2021. WMO Atlas of Mortality and Economic Losses from Weather, Climate and Water Extremes (1970–2019). WMO-No. 1267. https://library.wmo.int/doc_num.php?explnum_id=10989.

Xu, L., Chen, N., Zhang, X., 2019. Global drought trends under 1.5 and 2 °C warming. Int. J. Climatol. 39, 2375–2385. https://doi.org/10.1002/joc.5958.

Zambrano, F., Wardlow, B., Tadesse, T., Lillo-Saavedra, M., Lagos, O., 2017. Evaluating satellite-derived long-term historical precipitation datasets for drought monitoring in Chile. Atmos. Res. 186, 26–42. ISSN 0169-8095. https://doi.org/10.1016/j.atmosres.2016.11.006.

Zhang, Y., Wu, C., Yeh, P.J.F., Li, J., Hu, B.X., Feng, P., Jun, C., 2022. Evaluation and comparison of precipitation estimates and hydrologic utility of CHIRPS, TRMM 3B42 V7 and PERSIANN-CDR products in various climate regimes. Atmos. Res. 265 https://doi.org/10.1016/j.atmosres.2021.105881. ISSN 0169-8095.